

On the scribing and subsequent fracturing of silicon semiconductor wafers

A. MISRA, I. FINNIE

Department of Mechanical Engineering, University of California, Berkeley, California, USA

The integrated circuits deposited on silicon wafers are often separated by scribing with a diamond tool followed by bending to produce fracture. Using a commercial scribing tool we find permanent deformation and three types of crack. The median crack which propagates downwards is the objective of the scribing process. Lateral cracks which form, apparently following plastic deformation, may lead to chipping on either side of the scribing tool. These cracks and also the chevron cracks which form on the surface are very similar to cracks observed in scratching glass. However, in silicon, because of its anisotropy, the chevron cracks may be a serious problem since they can guide the median crack out of the scribing direction onto a preferred cleavage plane. This aspect leads to a brief discussion of the crystallography of silicon and recommendations for scribing configurations which should minimize undesired fracture. Finally, it is shown that the established methods of linear elastic fracture mechanics may be used to predict the maximum radius of curvature required to fracture a wafer containing a prescribed series of median cracks.

1. Introduction

Over the past few years the development of "Large Scale Integrated Circuits" represents a quantum leap in the technology of mankind. Typically, some 250 chips are made from one 0.15 to 0.5 cm thick, precisely polished single crystal silicon wafer about 8 cm in diameter. The spacing between the circuits is typically 0.05 mm, and to separate individual chips from the wafer a variety of techniques have been used. These include laser beams, diamond saws and scribing with a single-point diamond tool. The latter process of scribing by drawing the tool across the wafer to produce a crack, which is subsequently propagated by bending, is an attractive one in that it is cleaner than laser vaporization of material or sawing with a coolant. However, there is often a significant wastage in this simple mechanical process because the silicon wafer may not break along the desired path.

Compared to the extensive work which has been reported on the electronic aspects of silicon

chips, relatively little attention appears to have been given at a research level to the mechanical problems involved in separating the chips from the parent wafer. For this reason, in the present paper we examine the process of scribing and bending of silicon wafers. It is shown that information in the literature provides help in interpreting the fracture patterns developed under scribing tools. Possible improvements in the scribing process are discussed, and it is shown that the application of fracture mechanics may be of value in determining the radius of curvature required to propagate cracks across the wafer.

2. The scribing process

When materials that we describe normally as "brittle" are loaded on small regions by indenters or cutting tools they may exhibit ductile behaviour. In essence, this occurs because the probability of finding a large strength-impairing flaw in a small region is low. As a result, the average fracture stress increases for small regions (the "size

effect”) and plastic deformation may occur before fracture. This transition from brittle to ductile behaviour is enhanced if the stress state under the indenter or tool is largely triaxial compression, for this will inhibit fracture while having no influence on the shear stress required for plastic deformation. For these reasons, as the load on the tool, which influences the size of the stressed region, or the tool geometry, which influences the stress state, are changed, several different types of behaviour may be observed. At one extreme with large indenters and large loads only elastic behaviour is observed prior to fracture. For example, under static vertical loading the familiar Hertzian cone crack is observed under a spherical indenter while radial cracks may occur near a sharp indenter or with a spherical indenter at large loads. At the other extreme at very low loads it is easy to demonstrate, at least for glass, that a “chip” may be removed or a groove may be formed without material removal, depending on the tool geometry. Neither of these two extremes, purely brittle behaviour or purely ductile behaviour, appears to be suitable for scribing where the objective is to produce a crack normal to the surface of the wafer.

Although scribing has received little attention [1, 2], the related problem of indenting brittle solids with sharp indenters has been studied in detail. A review by Lawn and Wilshaw [3] provides a summary of this work. A significant result for our present study is the observation by Lawn and Swain [4] of the crack patterns which form when plastic deformation occurs under a sharp indenter. On loading, the median crack sketched in Fig. 1a is formed. On unloading, the residual stresses due to plastic deformation lead to lateral cracks which start below the surface and may propagate to the surface to remove a chip. The case of the blunt indenter, i.e. a sphere, has been examined in great detail. The situation most often studied, that of normal contact which leads to Hertzian cone cracks [5, 6] is not particularly relevant to the present study. The case of cracking due to sliding a sphere across a brittle solid is of some interest [7–9]. Here the cracks which form behind the moving indenter are partial cones [9]. They appear as a series of “horseshoes” on the surface opening towards the direction of sliding as sketched in Fig. 1b.

To study the crack pattern produced in commercial scribing operations we used equipment

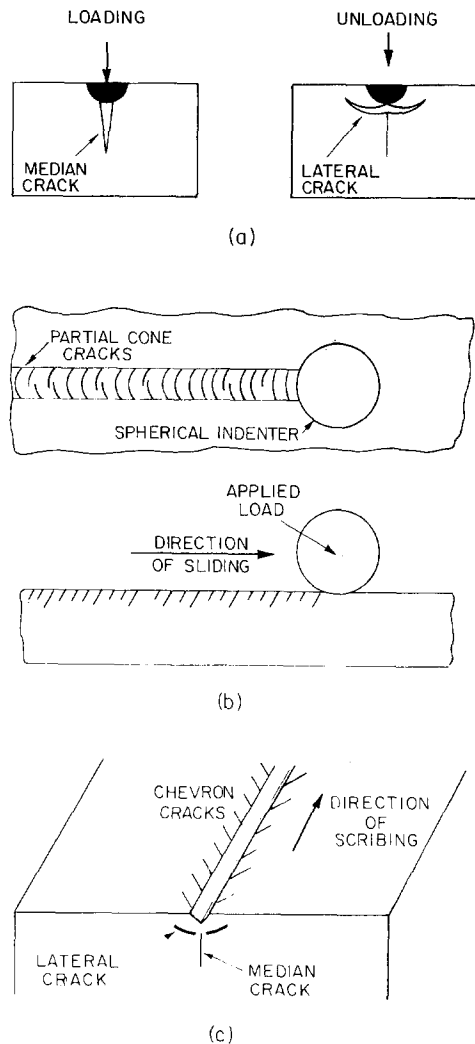


Figure 1 Schematic drawings of (a) the median and lateral cracks formed due to a sharp indenter, (b) the partial cone cracks formed due to scribing by a spherical indenter, (c) the median, lateral and chevron cracks formed due to scribing by a sharp indenter.

made available by Loomis Industries, Inc. of St Helena, California. The details of the parts of the scribing diamond which contact the surface are shown in Fig. 2. Examination of the scribing process by optical microscopy, as shown in Fig. 3, provides limited information. The tool produces a groove with “chevron” cracks opening in the direction of tool travel. The higher magnification and depth of focus possible with scanning electron microscopy provides a much clearer picture of the scribing process. Fig. 4 shows that the tool has produced a plastically deformed groove. No “chips” or debris corresponding to material removal by ductile cutting were observed, and one

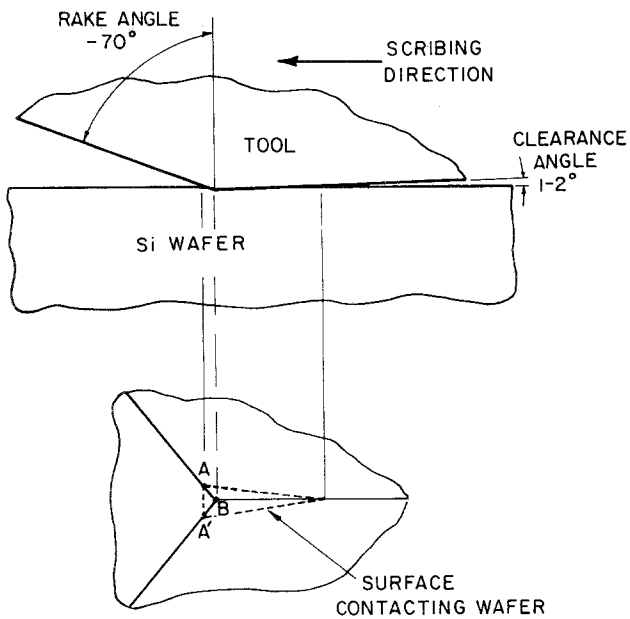


Figure 2 Geometrical details of tool used to scribe silicon wafers.

would not expect chip formation for this large negative rake angle. The chevron cracks appear to start at the rim of the plastically deformed region. To obtain information about the subsurface damage the wafer was scribed in a direction perpendicular to the original direction and then broken.

Fig. 5 shows the fracture under the initial scribe line which we can only assume was not influenced by fracture along the second scribe line. The median and lateral cracks which we have also shown schematically in Fig. 1c are strikingly similar to those observed by Lawn and Swain [4] under

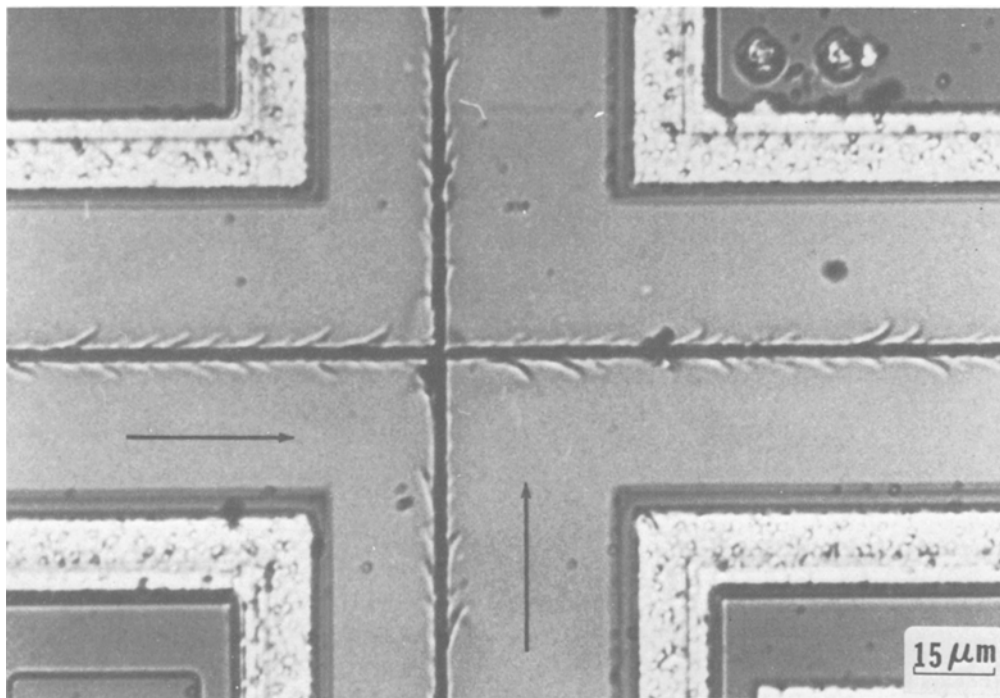


Figure 3 Optical microscope photograph showing chevron cracks on the silicon wafer surface. Arrows show the direction of scribing. (Photograph supplied by Mr. J. Loomis).

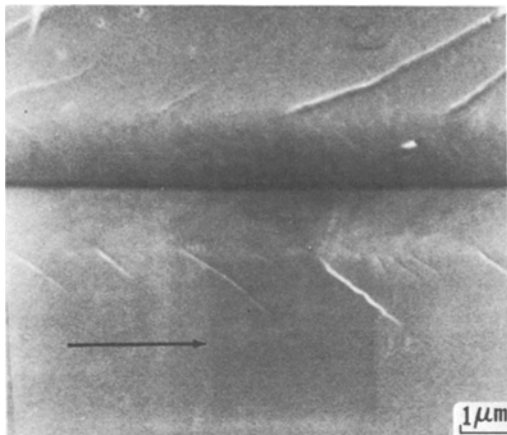


Figure 4 SEM photograph showing chevron cracks on the silicon wafer surface. Arrow shows the direction of scribing.

a Knoop indenter. Recently Swain [10] has summarized the results of scratching tests on glass using Vicker's indenters, and again fracture patterns very similar to that in Fig. 5 are observed.

The median crack is the objective of the scribing process since it is propagated by bending to separate the wafer. An approximate expression for the depth of the median crack produced under a static Vicker's indenter has been given by Lawn and Swain [4] while Swain [10] has also considered the moving Vicker's indenter. These analyses are useful in indicating the variables which control the depth of the median crack. However, precise quantitative prediction of median crack depth for a tool such as shown in Fig. 2 does not appear possible at the present time. For this reason we refer to experiment, such as shown in Fig. 5, to obtain the depth of the median crack.

Lateral cracks if confined in extent should not present a problem since the material removed as they propagate to the surface is away from the electronic portion of the chip. However, as we will see later in discussing the crystallography of silicon, the chevron cracks may cause difficulty by guiding the median cracks out of the scribing direction and into a preferred cleavage plane. For this reason, it would be desirable to have more information on the factors governing the formation of chevron cracks. They do not appear to be associated with the crystallography of silicon for, as seen in Fig. 3, they form, whether scribing is carried out along a preferred cleavage plane or at 30° to this direction. Also, they have been observed in glass and other brittle materials [1, 2, 11, 12].

Badrick, *et al.* [2] have attempted to explain chevron cracks by invoking the analysis of "horse-shoe" cracks produced by sliding spherical indenters. However, the large amounts of plastic deformation occurring in scribing should invalidate any elastic analysis. Also, chevron cracks form ahead of the tool while horseshoe cracks initiate behind the indenter. Rather, it appears that large tensile stresses will be produced at the sharp corners A in Fig. 2 where the tool contacts the surface. Moving down the leading corners of the tool (AB in Fig. 2), one would expect an increased hydrostatic compression and less tendency for cracking. We have not pursued the influence of tool shape and depth below surface on chevron cracking but these topics appear to be worth further attention.

3. Some crystallographic considerations

Most of the silicon wafers used in the semiconductor industry are grown such that their surface is a (111) plane. In a pure silicon crystal the natural cleavage plane is $\{111\}$; that is, the crystal will fracture along $\{111\}$ planes most easily. Besides the surface (111) plane, the wafer has three more $\{111\}$ planes which intersect the surface plane in $\langle 110 \rangle$ directions (Fig. 6), to form an equilateral triangle on the surface of the wafer.

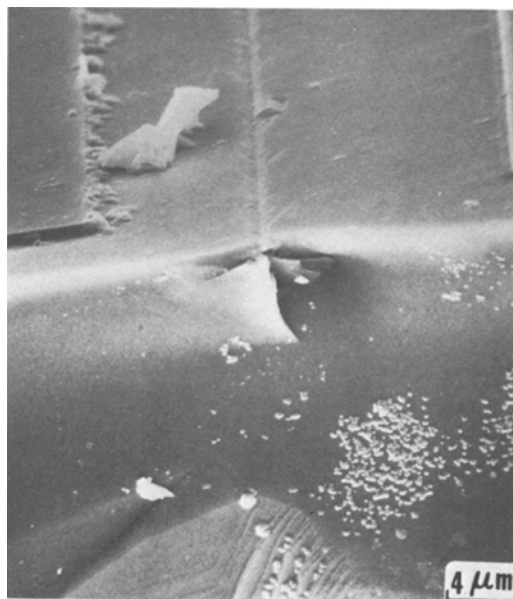


Figure 5 SEM photograph showing median and lateral cracks below the scratch. Initial scratch is in $\langle 110 \rangle$ direction. The second scratch, which later was propagated by bending, is in the $\langle 112 \rangle$ direction with fracture on a $\langle 110 \rangle$ plane.

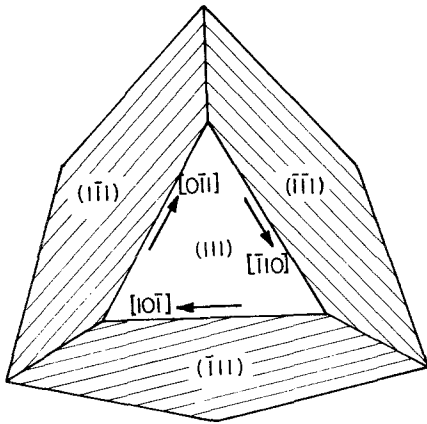


Figure 6 $\{111\}$ cleavage plane in silicon crystal.

For a rectangular chip to be cut from the wafer, two of its sides should be scribed along the $\langle 110 \rangle$ direction for easy breakage. The other two sides of the rectangle will be scribed along the $\langle 11\bar{2} \rangle$ direction which is normal to the $\langle 110 \rangle$ direction. The wafer will break easily along the $\langle 110 \rangle$ direction because here the fracture occurs along the $\{111\}$ natural cleavage plane. However, along the $\langle 11\bar{2} \rangle$ direction the crack follows the $\{110\}$ plane which has a higher surface energy than the $\{111\}$ plane and is more difficult to fracture. During dicing the wafer breaks perfectly along the easy $\langle 110 \rangle$ direction, but while breaking along the $\langle 11\bar{2} \rangle$ direction, the crack occasionally follows the chev-

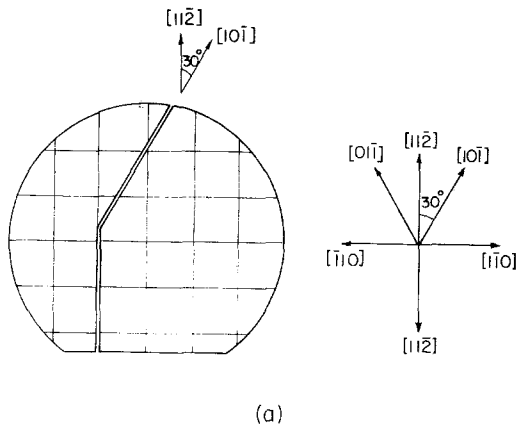
ron crack formed during the scribing and tilts towards the nearest $\langle 110 \rangle$ direction which is at 30° to the $\langle 11\bar{2} \rangle$ direction, thus spoiling many circuits (Fig. 7).

It can be seen that this problem is inherent in the crystal structure of silicon. It can break easily in the $\langle 110 \rangle$ direction but is difficult to break in the $\langle 11\bar{2} \rangle$ direction. Attempts to improve tool design may minimize this problem by limiting the chevron cracks but may not eliminate it.

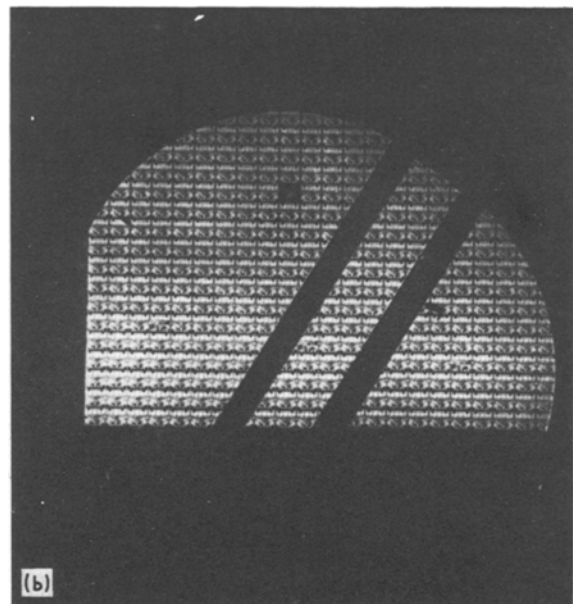
It is proposed that instead of making the semiconductor circuits rectangular they should be made in the shape of a rhombus with one angle 60° (Fig. 8) or an equilateral triangle, with the sides lying along the $\langle 110 \rangle$ directions. By doing so, fracture will occur along the natural cleavage plane $\{111\}$ which should increase significantly the efficiency of the dicing process. However, such a solution may not be appealing to the circuit designer for other reasons.

4. An application of fracture mechanics

Usually the wafers are separated into chips, after scribing, by being bent to a prescribed radius of curvature. Normally, this is done first to produce fracture in the difficult or $\langle 11\bar{2} \rangle$ direction, and then the wafer is turned 90° and bent to produce fractures in the easy or $\langle 110 \rangle$ direction. Selection of the appropriate radius of curvature is important because too large a radius may not propagate all



(a)



(b)

Figure 7 Breakage of silicon wafer along the undesired $[10\bar{1}]$ direction while trying to break along the $[11\bar{2}]$ direction.

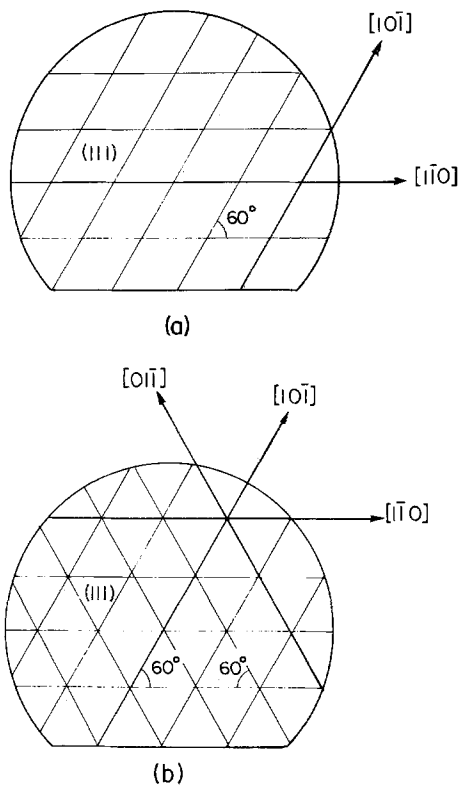


Figure 8 Proposed shapes for integrated circuits.

the median cracks while too small a radius may propagate smaller inherent cracks introduced by the process of circuit preparation. An upper limit on the radius of curvature required may be estimated if we idealize the scribed wafer as shown in Fig. 9. Lateral and chevron cracks are neglected and the median cracks of depth a are assumed to be far enough apart so that their interaction can be ignored. Using the procedure described in the Appendix, it is then possible to calculate the radius of curvature R at which cracks of given depth a will

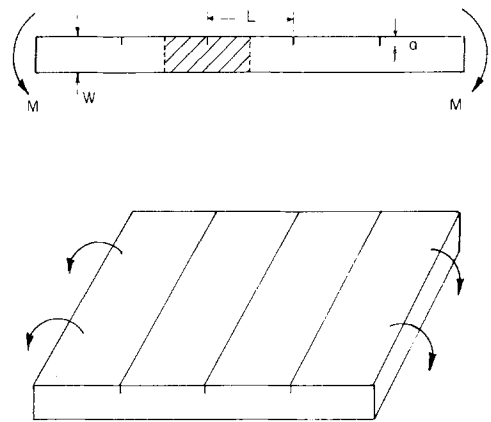


Figure 9 Dicing of silicon wafer by bending. The shaded region of length L is used to predict the radius of curvature required for fracture.

propagate. Fig. 10 shows the result for a crack spacing L of 2.5 mm and wafers of thickness $W = 0.5$ and 0.25 mm. The predictions are based on limited information on the fracture properties for the (111) plane of silicon in the "easy" or $\langle 110 \rangle$ direction. They could be modified for fracture in the "difficult" direction when more information on fracture properties is available. However, the general behaviour shown is of interest. Taking the median crack depth $a \approx 0.0125$ mm from Fig. 4 the dimensionless values of $\alpha = a/W$ for the two wafer thicknesses are shown in Fig. 10. We find a maximum radius of about 30 cm for the 0.5 mm thick wafer and about 14 cm for the 0.25 mm wafer. Much smaller radii should be avoided for they would lead to the propagation of very small cracks such as might be produced in the fabrication process.

If cracks grew under equilibrium conditions, Fig. 10 suggests that arrest should occur just before $\alpha = 1.0$. However, during the period of

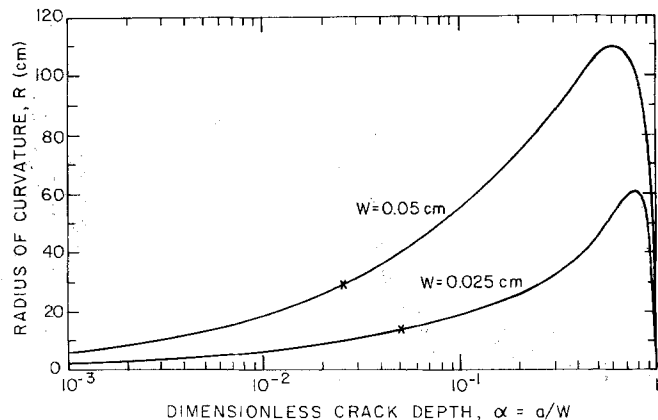


Figure 10 Plot of radius of curvature (R) needed to propagate a median crack versus α (ratio of crack length to the thickness of the wafer). Crosses correspond to a crack of depth 0.0125 mm.

crack growth after initiation, the radius of curvature for initiation is less than that required for larger values of crack length. As a result, more energy will be released by fracture than can be absorbed. This excess energy appears as kinetic energy. If we assume that some fraction of the kinetic energy must be absorbed by the fracture process before the crack can arrest, it seems probable that the crack will not stop at some value $0.9 < \alpha < 1.0$ but rather will propagate across the wafer. In this connection, too small a radius of curvature will result in a larger amount of kinetic energy in the chips and hence a greater likelihood of crack branching or disruption of the array of chips.

5. Conclusions

There appears to be many aspects of the scribing of silicon and other brittle solids which could be clarified by further study. We have pointed out that it is important to eliminate chevron cracks and minimize lateral cracks while producing deep median cracks. Improved chip separation may be possible by departing from the traditional rectangular shape but this may not be attractive for other reasons. Finally, the well-developed procedures of linear elastic fracture mechanics may be useful in designing equipment to fracture the scribed wafers in an optimum manner.

Appendix

The radius of curvature required for median crack propagation

We consider the rectangular plate shown in Fig. 9 and isolate a section of length L containing a central crack of depth a . It is convenient to divide a by the plate thickness W to obtain a dimensionless crack length $\alpha = a/W$. If M is the bending moment per unit width of plate, the outer fibre stress in the absence of a crack and the stress intensity factor are given by

$$\sigma = 6M/W^2 \quad (A1)$$

$$K_I = \sigma\sqrt{(\pi a)F(\alpha)} \quad (A2)$$

Since $L/W = 10$ and 5 for the cases we are considering, it is reasonable to treat each crack as isolated from the others and use the solution given

by Tada *et al.* [13]:

$$F(\alpha) = \left[\sqrt{\left(\frac{2}{\pi\alpha} \tan\left(\frac{\pi\alpha}{2}\right) \right)} \right] \times \left[\frac{0.923 + 0.199(1 - \sin(\pi\alpha/2))^4}{\cos(\pi\alpha/2)} \right]$$

This is said to be within 0.5% of the exact solution for $0 \leq \alpha < 1.0$. The same reference gives the angle of deflection between the two ends due to the crack for plane strain as

$$\theta_{\text{crack}} = \frac{4\sigma(1-\nu^2)}{E} S(\alpha) \quad (A3)$$

where

$$S(\alpha) = \left(\frac{\alpha}{1-\alpha} \right)^2 [5.93 - 19.69\alpha + 37.14\alpha^2 - 35.84\alpha^3 + 13.12\alpha^4]$$

is said to be within 1% for $0 \leq \alpha < 1$ and E and ν are Young's Modulus and Poisson's Ratio.* Using Equation A2 we may eliminate σ from Equation A3 to obtain

$$\theta_{\text{crack}} = \frac{4K_I(1-\nu^2)}{E\sqrt{(\pi W)}} \left[\frac{1}{\sqrt{\alpha}} \frac{S(\alpha)}{F(\alpha)} \right] \quad (A4)$$

The angle of deflection of one end relative to the other in an uncracked plate is

$$\theta_{\text{no crack}} = \frac{12ML(1-\nu^2)}{EW^3}$$

Using Equations A1 and A2 this becomes

$$\theta_{\text{no crack}} = \frac{2K_I L(1-\nu^2)}{EW^{3/2}\sqrt{(\pi\alpha)F(\alpha)}} \quad (A5)$$

The total angular deflection required to propagate the crack is obtained by adding Equations A4 and A5 and replacing K_I by K_{Ic} the plane strain fracture toughness

$$\theta = \theta_{\text{crack}} + \theta_{\text{no crack}} = \frac{K_{Ic}(1-\nu^2)}{E} \left\{ \frac{4}{\sqrt{(\pi\alpha W)}} \frac{S(\alpha)}{F(\alpha)} + \frac{2L}{W^{3/2}\sqrt{(\pi\alpha)F(\alpha)}} \right\} \quad (A6)$$

The radius of curvature of the plate shown in Fig. 9 is given by $R = L/\theta$ and can be evaluated

*In [13], the expression for $S(\alpha)$ shows $+ 35.84\alpha^3$, which appears to be an error.

from Equation A6 for specific values of K_{Ic} , E , ν , α , W and L .

We have taken values of $K_{Ic} = 9.37 \times 10^2$ N cm^{-3/2} for the {111} plane, $E = 15.6 \times 10^6$ N cm⁻² and $\nu = 0.215$ reported by St John [14]. Also, choosing $L = 0.25$ cm, $W = 0.025$ cm and 0.05 cm leads to the curves shown in Fig. 10. We have presented the results in a semi-logarithmic plot to expand the region corresponding to small values of α .

Acknowledgement

Mr James Loomis of Loomis Industries, St Helena, California, provided the material and equipment for our scribing tests. We are grateful to him also for drawing our attention to the problems involved in the scribing process.

References

1. J. D. B. VELDKAMP and R. J. KLEIN WASSINK, Philips Res. Repts. 31 (1976) 153.
2. A. S. T. BADRICK, F. ELDEGHAIY, K. E. PUTTICK and M. A. SHAHID, *J. Phys. D: Appl. Phys.* 10 (1977) 197.
3. B. R. LAWN and R. WILSHAW, *J. Mater. Sci.* 10 (1975) 1049.
4. B. R. LAWN and M. V. SWAIN; *ibid.* 10 (1975), 113.
5. F. C. FRANK and B. R. LAWN, *Proc. Roy. Soc. A299* (1967) 291.
6. I. FINNIE and S. VAIDYANATHAN, "Fracture Mechanics of Ceramics" (Plenum Press, New York, 1974) p.231.
7. B. R. LAWN, *Proc. Roy. Soc. A299* (1967) 307.
8. G. M. HAMILTON and L. E. GOODMAN, *J. Appl. Mech.* 33 (1966) 371.
9. B. BETHUNE, *J. Mater. Sci.* 11 (1976) 199.
10. M. V. SWAIN, "Fracture Mechanics of Ceramics", Vol. 3, to be published by Plenum, New York.
11. A. BROESE VAN GROENOU, N. MAAN and J. D. B. VELDKAMP, Philips Res. Repts. 30 (1975) 320.
12. J. M. POWERS, R. G. CRAIG and K. C. LUDEMA, *Wear* 23 (1973) 141.
13. H. TADA, P. PARIS and G. R. IRWIN, "The stress Analysis of Cracks Handbook" (Del Research Co., Hellertown, Pa., USA, 1973)
14. St. JOHN, Ph. D. Thesis, University of California, Berkeley, 1971.

Received 12 and accepted 26 January 1979.